ELSEVIER

Polymer 41 (2000) 9283–9290

polymer

www.elsevier.nl/locate/polymer

# Phase structure of ternary polypropylene/elastomer/filler composites: effect of elastomer polarity

K. Premphet*, P. Horanont

*Department of Chemistry, Mahidol University, Rama VI Road, Bangkok 10400, Thailand*

Received 9 August 1999; accepted 6 April 2000

## Abstract

Phase structure of ternary polypropylene/elastomer/calcium carbonate composites has been investigated using scanning electron microscopy, dynamic mechanical analysis and differential scanning calorimetry. Two kinds of phase structure were observed either a separate dispersion of the phases or encapsulation of the filler by elastomer. The composite phase structure was determined mainly by the chemical character of the components and, to a lesser degree, by the mixing sequences of each component. In this study, the use of non-polar ethylene–octene copolymer (EOR) resulted in a composite having separate dispersion of elastomer and filler particles. When a polar ethylene–vinyl acetate (EVA) elastomer was used, an encapsulation structure was formed. This is attributed to the higher affinity of EVA to calcium carbonate. Analysis of the composite structure formed, using the Geometric Mean approach was found to be useful as a qualitative technique.

*Keywords*: Polypropylene; Ternary composites; Phase structure

## 1. Introduction

Ternary phase polymer composites containing soft elastomer and rigid filler have become the subject of an increasing number of studies that aim to achieve an optimum balance of impact strength and stiffness. Various fillers have been employed in ternary phase polymer composites. These include talc [1–3], calcium carbonate [4–10] and kaolin [11–13]. The most commonly used elastomers are ethylene–propylene copolymer (EPR) and ethylene–propylene diene terpolymer (EPDM). The mechanical properties of such composites are determined not only by their composition and the characteristics of the components, but also by the phase morphology present, and in particular, the relative dispersion of additive components. In ternary phase composites, two types of phase structure may be formed: separate dispersion where the elastomer and filler particles are dispersed separately in the polymer matrix [7,14,15]; or encapsulation where the elastomer encapsulates the filler particles [4,16], resulting in a low modulus interlayer between the matrix and filler.

Thermodynamic analysis of these two types of phase structure revealed that encapsulation is the thermodynamically favoured process [6]. However, the final structure was reported to be determined by the adhesion between phases and the stability of the encapsulated units against shear forces in the melt during the mixing process [6]. Thus the phase structure of ternary phase composites is influenced by the melt rheology of the system, compounding techniques, and the surface characteristics and mutual wettability of the fillers and polymer components. In PP/EPDM/calcium carbonate composites, surface treatment of filler was found to result in a separate dispersion of phases, whereas encapsulation occurred when untreated calcium carbonate was used [4,5]. To promote the adhesion between the polymer and filler particles, functionalisation of polymer phases was carried out. In PP/EPR/filler systems, it was shown that incorporating PP functionalised with maleic anhydride resulted in separate dispersions of elastomer and filler. Using maleated EPR and nonfunctionalised PP gave a filler encapsulation structure [7,8].

The objective of the present study was to investigate the effect of elastomer polarity on the phase structure of ternary PP composites containing calcium carbonate filler. The non-polar and polar elastomers examined were ethylene–octene copolymer (EOR) and ethylene–vinyl acetate (EVA), respectively. EOR and EVA are both structurally similar in the sense that both are copolymers of a non-polar backbone, but EVA also contains the polar acetate group. The higher polarity of EVA will result in a higher affinity for

---

* Corresponding author.

PII: S0032-3861(00)00303-7

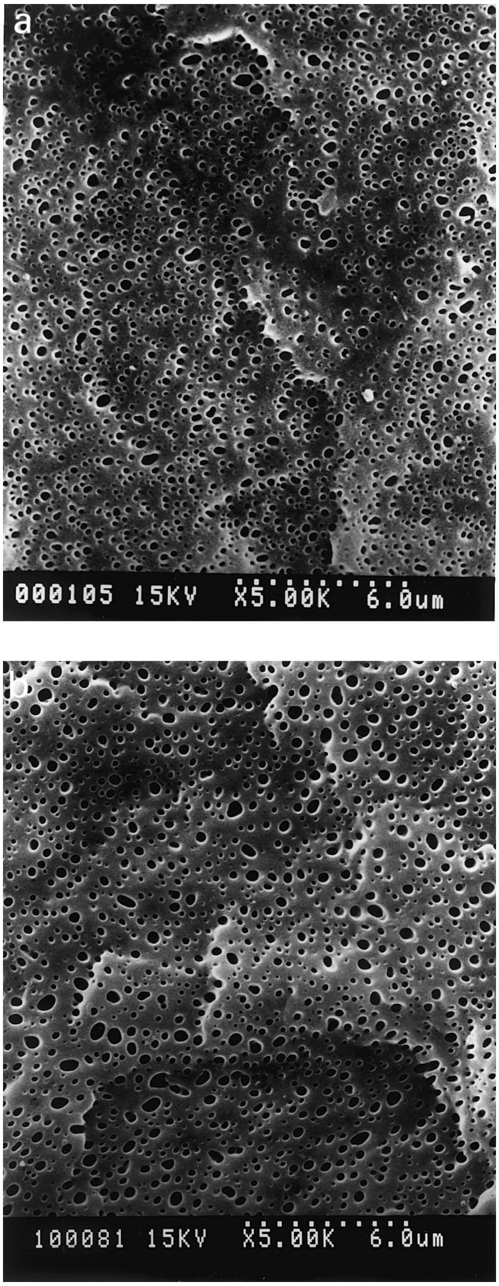

Fig. 1. Cryogenic fractured and etched surfaces of binary blends. (a) PP/EOR (70/30); and (b) PP/EVA (70/30).

calcium carbonate, and is therefore expected to give a composite with an encapsulation structure. While the non-polar EOR should lead to a separate dispersion structure.

## 2. Experimental

### 2.1. Materials

The base material for the composites was polypropylene (PP) homopolymer P400S [melt flow rate (MFR) = 4.13 g/10 min] supplied by Thai Polyethylene Co. The two elastomers used were EOR Engage 8150 consisting of 25 wt.% octene with a MFR of 0.5 g/10 min, and EVA Elvax 460 having 18 wt.% vinyl acetate and a MFR of 2.4 g/10 min. Both are products of Dupont Dow Elastomer Co. The filler used was untreated calcium carbonate ($CaCO_3$) grade Microcal (Lime Quality Co.), with a median diameter in the range of 2–5 μm.

### 2.2. Compounding

The ternary composites of PP/elastomer/$CaCO_3$ were prepared in a co-rotating twin screw extruder (Prism TSE 16) using a barrel temperature profile of 160–200°C (from feed zone to die). Samples were produced at a screw speed of 220 rpm, giving a throughput rate of 3 kg/h. In this study, the effect of the sequence in which the components (PP, EOR or EVA, $CaCO_3$) were mixed in the extruder was also investigated. Two different procedures were used. In the first procedure, PP and filler were meltmixed at first and subsequently blended with either EOR or EVA to produce RC1 and VC1 composites. While the RC2 and VC2 composites were prepared by mixing filler with EOR and EVA, prior to blending with PP.

### 2.3. Phase structure analysis

The phase structures of the composites were examined by scanning electron microscopy. Specimens were prepared by immersing impact test pieces in liquid nitrogen, before fracturing them using an impact-testing machine. To improve contrast between the PP matrix and elastomer phases (EOR or EVA), the fractured surfaces were exposed to hot heptane vapour for 20 s. in order to remove the elastomer particles from the composites. The surfaces prepared in this way were platinum/palladium sputtercoated and examined in a Hitachi S2500 scanning electron microscope.

The melting and crystallisation behaviour of the composites was studied using a Perkin–Elmer DSC-7 differential scanning calorimeter. Samples were first heated from 50 to 230°C at a scan rate of 10°C/min and then maintained at 230°C for 5 min before cooling to 50°C at the same rate.

The dynamic mechanical properties of selected composites were determined using a Polymer Laboratories Dynamic Mechanical Thermal Analyser. Testing was carried out in bending mode over a temperature range of −100 to 120°C at a frequency of 6.28 rad/s (1 Hz).

Surface tension of polymers was determined by contact angle measurements at room temperature using a Kruss model G1 contact angle meter. The single liquid method using water and methylene iodide as reference liquids was employed. The surface tension ($\gamma$) of the polymers was obtained from a combination of the dispersion ($\gamma_d$) and polar ($\gamma_p$) components of the surface tension.

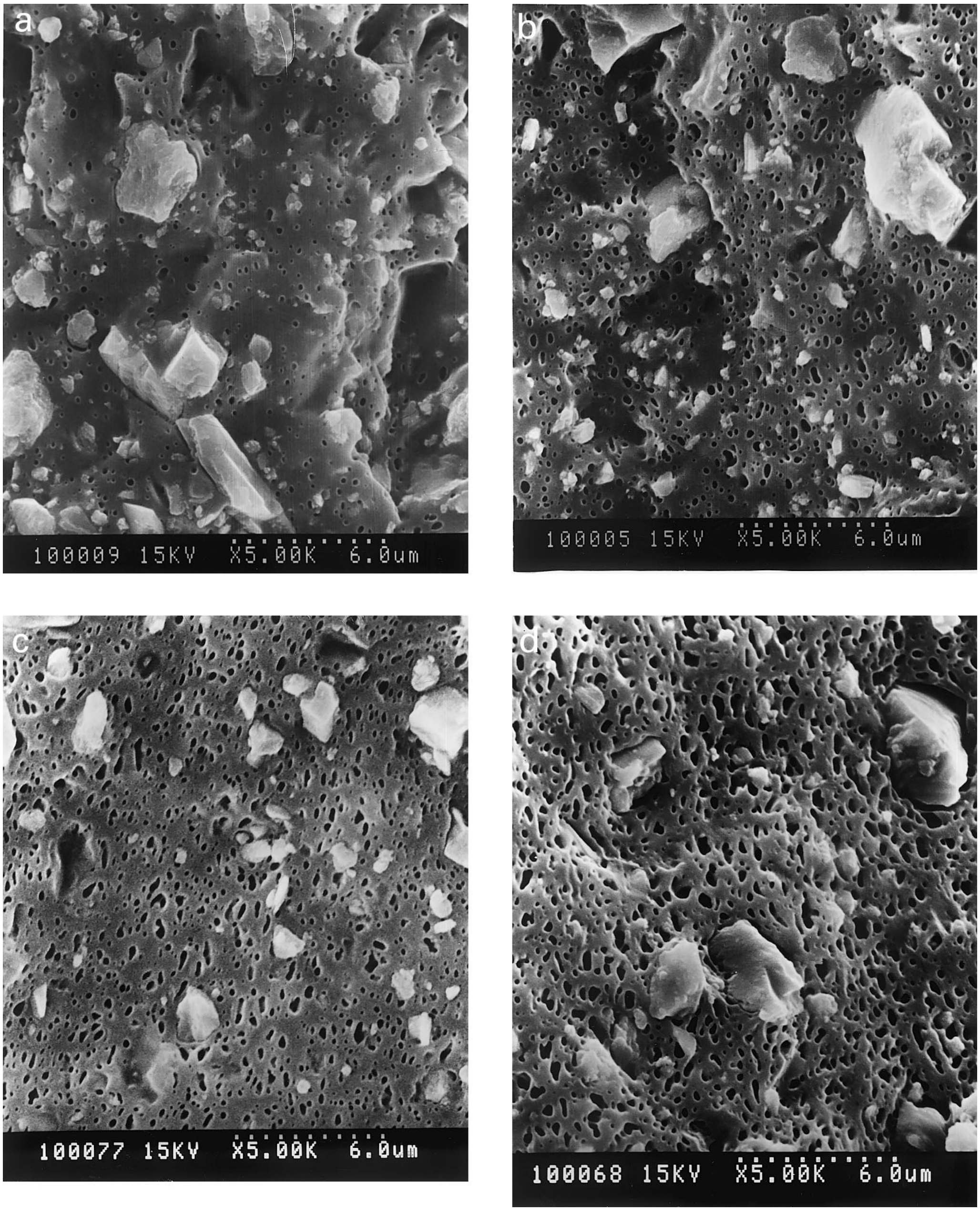

Fig. 2. Cryogenic fractured and etched surfaces of ternary PP/EOR/$CaCO_3$ composites. (a) 60/10/30; (b) 60/20/20; (c) 60/30/10 (RC1 composite); and (d) 60/30/10 (RC2 composite).

## 3. Results and discussion

### 3.1. SEM analysis

SEM micrographs of the etched cryogenic fracture surfaces of PP/EOR and PP/EVA binary blends are shown in Fig. 1. The dark holes represent the elastomer droplets, which are dissolved out by selective etching. The two-phase morphology is clearly visible in both systems. The dispersion of elastomer droplets is quite fine and uniform in size. The droplet size of EOR is in the range of 0.04–0.41 μm that is slightly smaller than that of EVA (0.04–0.63 μm). In the case of ternary composites; however, different phase microstructures were formed depending on whether the EOR or EVA was incorporated. Fig. 2 reveals the microstructure of PP/EOR/$CaCO_3$ composites, where EOR and $CaCO_3$ particles were dispersed separately in the PP matrix. An increase of EOR content in the composite did not change this structure but increased the number density of dispersed EOR droplets in the PP matrix. By changing the sequence in which the PP, EOR and $CaCO_3$ were mixed, a fully encapsulation structure could not be achieved. In the system where EOR was prior mixed with $CaCO_3$ (RC2 composite), a separate dispersion of EOR and $CaCO_3$ in the PP matrix

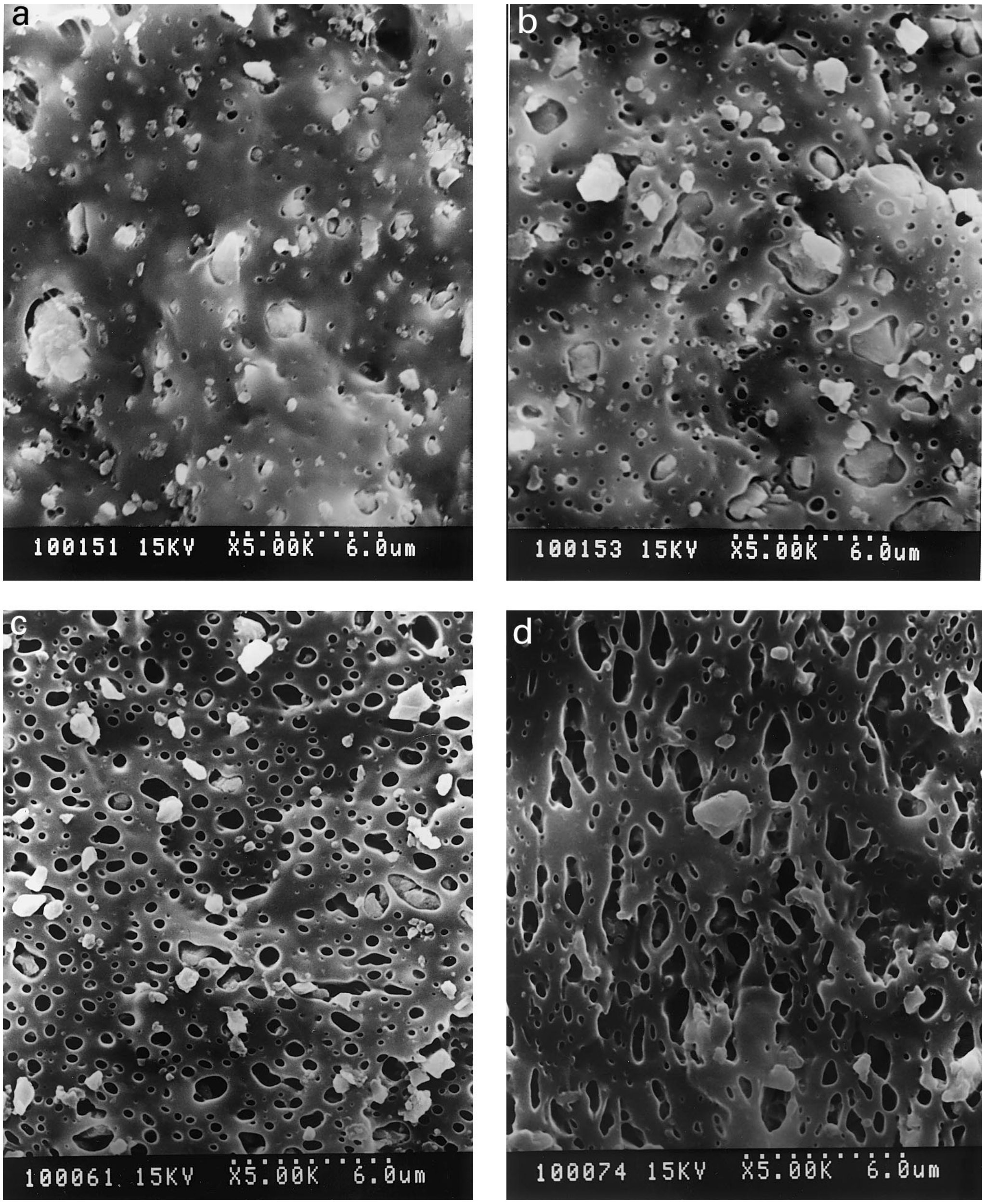

Fig. 3. Cryogenic fractured and etched surfaces of ternary PP/EVA/$CaCO_3$ composites. (a) 60/10/30; (b) 60/20/20; (c) 60/30/10 (VC1 composite); and (d) 60/30/10 (VC2 composite).

was again observed (Fig. 2d). However, there was some evidence to indicate that some filler particles in the composites were partially wetted by EOR. The EOR droplets in this composite were also found to be more elongated and larger in size compared to those of the RC1 composites where filler was prior mixed with PP (Fig. 2c).

A contrasting morphology is shown in Fig. 3 for the PP/EVA/$CaCO_3$ composite, where there is evidence of EVA encapsulation around the filler particles. The voids around the filler particles unambiguously indicated that elastomer was located at that place. It was also observed that at an EVA content of 10%, EVA was found almost completely in the interphase region (Fig. 3a). Isolated EVA droplets dispersed in the PP matrix was not apparent. Raising the elastomer content in the composites, the thickness of the interfacial layer did not increase and the elastomer appeared as a separate phase finely dispersed in the polymer matrix (Fig. 3b and c). The structure of PP/EVA/$CaCO_3$ composites is also independent of the sequence of mixing. The final structure remained of an encapsulation type (Fig. 3d), regardless of whether fillers were prior mixed with PP or with EVA. After etching, few clean $CaCO_3$ surfaces were observed in the sample prepared by prior mix filler with EVA (VC2 composite), but numerous separate holes, resulting from etching of the $CaCO_3$–EVA inclusions were present.

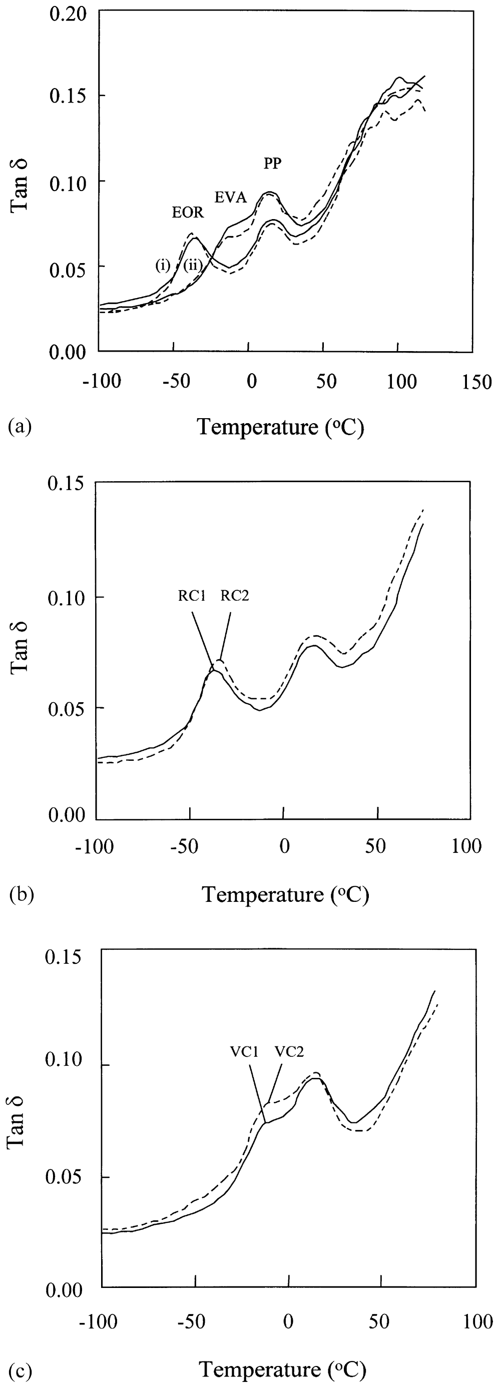

Fig. 4. Temperature dependency of tan $\delta$ at 1 Hz. for binary and ternary phase composites. (a) Temperature dependency of tan $\delta$ for binary (– – – –) and ternary (—) systems with EOR (i) and EVA (ii); (b) temperature dependency of tan $\delta$ for PP/EOR/$CaCO_3$ composites where the filler was prior mixed with PP (RC1) or with EOR (RC2); and (c) temperature dependency of tan $\delta$ for PP/EVA/$CaCO_3$ composites where the filler was prior mixed with PP (VC1) or with EVA (VC2).

### *3.2. Dynamic mechanical analysis*

The composite phase structure was also determined by the DMA technique. Fig. 4a shows the temperature dependency of tan $\delta$ at 1 Hz. for binary and ternary composites with EOR and EVA, in which the two tan $\delta$ peaks observed corresponded to the glass transition temperatures ($T_g$) of PP and the incorporated elastomers. In both systems the location of $T_g$ peaks of PP were the same at 15°C. The $T_g$ value of EOR in the ternary PP/EOR/$CaCO_3$ composites was also similar to that observed in the binary blend, indicating that $CaCO_3$ had no influence on the mobility of the EOR chains. This reflects a lack of association between EOR and $CaCO_3$ in this composite. In the PP/EVA/$CaCO_3$ composites, on the other hand, the shift of the EVA peak from $-17°$ (in the binary blend) to $-14$°C (in the ternary blend) was clearly seen. This suggested that, in this system, the incorporation of filler caused immobilisation of elastomer chains. Also, the DMA spectrum in Fig. 4a shows a much larger and broader elastomer transition in the PP/EVA/$CaCO_3$ than that of PP/EOR/$CaCO_3$ composites, because of the presence of filler in the elastomer phase in the former system. These results agree well with the SEM observations in which the phase structure of the composites in the former case was of an encapsulation type, while that of the latter was of a separate dispersion type. Similar results have been reported for PP/EPDM/$CaCO_3$ composite, where the presence of rubber around the filler particles broadened its glass transition and shifted it to a higher temperature [4,18]. The effect of mixing sequence on phase structure of PP/EOR/$CaCO_3$ and PP/EVA/$CaCO_3$ composites is shown in Fig. 4b and c, respectively. The composites prepared by mixing the elastomer and filler in the first stage (the RC2 and VC2 composites), show broader and stronger elastomer tan $\delta$ peaks. These peaks also shifted slightly to higher temperatures, indicating more immobilised elastomers in such composites. This confirms the previous SEM observations in which greater amounts of elastomer adhered to the filler particles in these composites.

### *3.3. Differential scanning calorimetry*

Table 1 summarises the differential scanning calorimetry (DSC) results for unmodified PP and its binary blends with either elastomer particles or calcium carbonate. An unmodified PP shows $T_c$ at 111°C and $T_{c\,\mathrm{onset}}$ at 115°C. Addition of EOR to PP scarcely changed the $T_c$ and $T_{c\,\mathrm{onset}}$ of PP while the addition of $CaCO_3$ led to a significant increase in both values. This implied that the incorporated filler had more influence on the crystallisation of PP than EOR. In ternary composites where both EOR and filler were incorporated (Fig. 5), the values of $T_c$ and $T_{c\,\mathrm{onset}}$ increased significantly as the filler concentration increased. From these results, it can be said that $CaCO_3$ acted as a nucleating agent promoting crystallisation of PP at its surface and hence led to a composite with higher $T_c$ and $T_{c\,\mathrm{onset}}$ values. The influence of $CaCO_3$ upon $T_c$ and $T_{c\,\mathrm{onset}}$ strongly indicated the direct contact between $CaCO_3$ and PP in the PP/EOR/$CaCO_3$ system. In other words, the structure in this composite was a separate dispersion. In the RC2 composites where

Table 1
Crystallisation temperature ($T_c$) and temperature of onset of crystallisation ($T_{c\ onset}$) of unmodified PP and its binary blends (60/40).

| Sample | $T_c$ (°C) | $T_{c\ onset}$ (°C) |
|---|---|---|
| PP | 111 | 115 |
| PP/EOR | 110 | 114 |
| PP/EVA | 110 | 113 |
| PP/$CaCO_3$ | 133 | 137 |

filler was prior mixed with EOR, a suppression of the nucleation efficiency of filler was observed. A decrease in $T_c$ and $T_{c\ onset}$ values is clear from Fig. 6.

In the case of PP/EVA/$CaCO_3$ composites, on the other hand, no influence of calcium carbonate on the $T_c$ and $T_{c\ onset}$ was observed (Fig. 5). The values of $T_c$ and $T_{c\ onset}$ of the PP/EVA/$CaCO_3$ system were constant even the filler concentration was increased up to 30 vol%. The loss of nucleating efficiency of filler in the EVA system is attributed to its encapsulation structure. As the filler particles in this system were surrounded by the EVA phase. The DSC experiments yielded results similar to those observed in the binary PP/EVA blends, without $CaCO_3$ present.

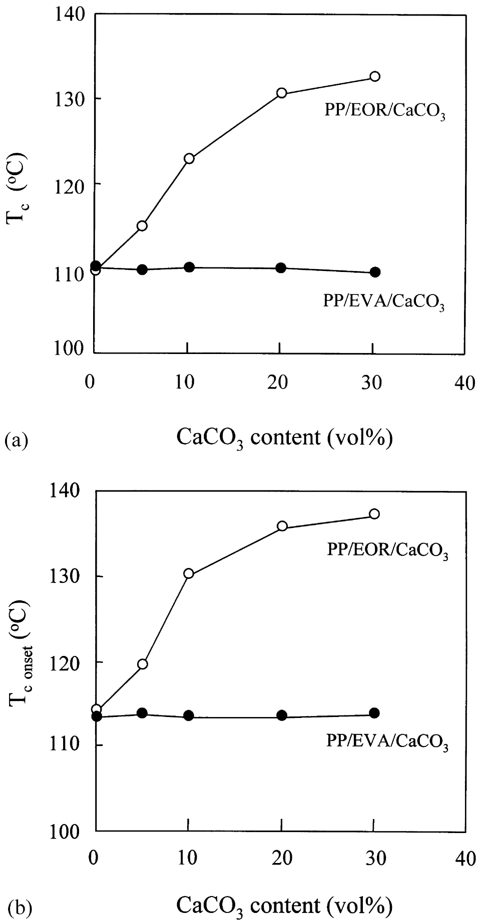

Fig. 5. Effect of filler contents on the crystallisation behaviour of ternary phase composites. (a) Effect on the crystallisation temperature ($T_c$); and (b) effect on the onset temperature of crystallisation ($T_{c\ onset}$). W, Composites containing EOR. X, Composites containing EVA.

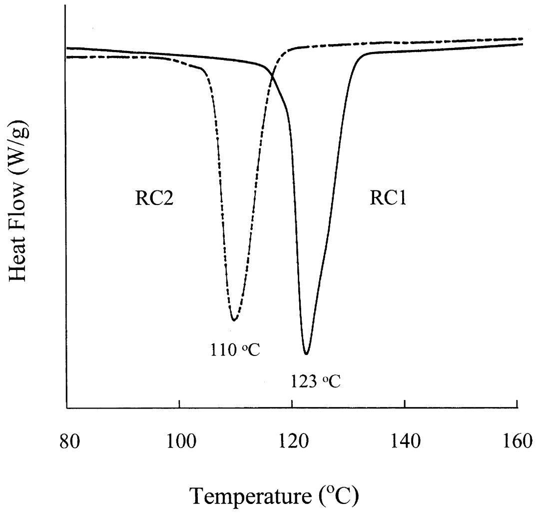

Fig. 6. DSC thermograms of PP/EOR/$CaCO_3$ composites. —, Composite prepared by prior mix the filler with PP (RC1). – – – –, Composite prepared by prior mix the filler with EOR (RC2).

### 3.4. Analysis of phase structure formation

The formation of particular phase structures depends on several factors. However, the limits of ideal structure have been reported to be determined by thermodynamic considerations [6]. Pukanszky et al. [6] analysed the processes taking place during the preparation of PP/EPDM/$CaCO_3$ composites and found that the final structure of such composites was determined by several factors including the free energy change of the process, the adhesion between phases, the viscosity of the polymer melts and the shear rate during mixing. In this study, some of these parameters (the free energy change and the adhesion between phases) will be calculated numerically. Although it is extremely difficult to determine these parameters accurately, the data obtained does allow comparisons to be made between the different phase structures.

In the ternary PP/elastomer/$CaCO_3$ composites of this study, as mentioned earlier, two kinds of phase structures were formed—either separate dispersion of components or encapsulation of filler particles by elastomer. Both structures resulted in the formation of two new surfaces, PP/EOR, PP/$CaCO_3$ in the former and PP/EVA, EVA/$CaCO_3$ in the latter. When new surfaces and interfaces are created, the input of some energy is required and the system tends to acquire a morphology with a minimum total free energy [6]. The change of the surface free energy is proportional to the size of the new surfaces and to the interfacial tension. The latter can be calculated from the surface tension of the components using the geometric mean equation of Wu [17]:

$$\gamma_{AB} = \gamma_A + \gamma_B - 2(\gamma_A^d \gamma_B^d)^{1/2} - 2(\gamma_A^p \gamma_B^p)^{1/2} \tag{1}$$

Table 2
The surface tension and its dispersion and polar components of the materials under investigation

| Material | Surface tension (mJ/m$^2$) | | |
|---|---|---|---|
| | Total ($\gamma$) | Disperse component ($\gamma^d$) | Polar component ($\gamma^p$) |
| PP | 30.0 | 26.0 | 4.0 |
| EOR | 30.3 | 26.4 | 3.9 |
| EVA | 37.2 | 29.7 | 7.5 |
| $CaCO_3$ [20] | 207.9 | 54.5 | 153.4 |

where $\gamma_{AB}$ is the interfacial tension, $\gamma_A$ and $\gamma_B$ are the surface tensions of the two materials in contact, and *d* and *p* refer to the dispersion and polar contributions, respectively. The surface tension values of $CaCO_3$ used in this analysis were taken from the literature [20]. Also, in this study all composites were prepared in a twin screw extruder and structure developed during mixing at around 160–200°C. The surface tension of the polymers was determined from contact angle measurements at ambient temperature. Nevertheless, by considering this data a better understanding of phase structure formation in the ternary composites can be reached.

The surface tension and the dispersion and polar components of the materials used in this investigation are given in Table 2. The calculated interfacial tensions of all possible polymer/elastomer, polymer/filler and elastomer/filler pairs are shown in Table 3. A study of the data shows that in a PP/EOR/$CaCO_3$ composite, the interfacial tensions ($\gamma_{AB}$) for PP/$CaCO_3$ and EOR/$CaCO_3$ were similar. This means that both PP and EOR had similar tendency to encapsulate the filler particles. However, because of the lower viscosity and higher concentration of PP in the composition, filler particles were surrounded by PP resulting in a separate dispersion structure [15].

In the PP/EVA/$CaCO_3$ composite, on the other hand, the interfacial tension ($\gamma_{AB}$) of PP/$CaCO_3$ was much greater than that of EVA/$CaCO_3$. Thus, the morphology possessing the lowest free energy was when $CaCO_3$ particles were encapsulated by the elastomer layer and these filler-elastomer inclusions were embedded in the PP matrix. However, the final structure of the composite was determined also by the magnitude of adhesion between the forming filler-elastomer inclusions against the shear forces occurring during the mixing process. The shear forces tended to remove the elastomer layer from the filler surface (de-encapsulation) and would lead to a separated dispersion of filler and elastomer particles. To compare the magnitude of adhesion between phases in the composites, the thermodynamic work of adhesion ($W_{AB}$) was calculated using the following relationship [19].

$$W_{AB} = 2(\gamma_A^d \gamma_B^d)^{1/2} + 2(\gamma_A^p \gamma_B^p)^{1/2}. \tag{2}$$

The results (Table 3) show the difference in the adhesion between the polar (EVA) and non-polar (EOR) elastomer to the filler surface. The higher value of $W_{AB}$ in EVA systems reflected a strong elastomer-filler interaction and this, in turn, influenced the stability of the encapsulated units against shear forces during mixing. Hence, an encapsulation structure was finally found in the PP/EVA/$CaCO_3$ composites.

## 4. Conclusions

A study of ternary polypropylene/elastomer/calcium carbonate composites has shown that two kinds of phase structure were formed: either a separate dispersion of the phases or encapsulation of the filler by elastomer. The elastomer polarity showed a major influence on the phase structure of the composites. In this study, composites containing non-polar EOR showed separate dispersion of the elastomer and filler particles. The use of polar EVA elastomer resulted in composites with encapsulation structure. In such composites DMA results showed a much larger and broader elastomer transition compared to that of ternary composites with non-polar EOR. The presence of filler in the elastomer phase of the PP/EVA/$CaCO_3$ system was also evident from the

Table 3
The calculated interfacial tension ($\gamma_{AB}$) and work of adhesion ($W_{AB}$) for all possible polymer/elastomer, polymer/filler and elastomer/filler pairs

| System | Possible pairs | Interfacial tension ($\gamma_{AB}$) (mJ/m$^2$) | Work of adhesion ($W_{AB}$) (mJ/m$^2$) | Final phase structure |
|---|---|---|---|---|
| PP/EOR/$CaCO_3$ | PP/EOR | 0.002 | 60.30 | Separation |
| | PP/$CaCO_3$ | 113.07 | 124.83 | |
| | EOR/$CaCO_3$ | 113.42 | 124.78 | |
| PP/EVA/$CaCO_3$ | PP/EVA | 0.67 | 66.53 | Encapsulation |
| | PP/$CaCO_3$ | 113.07 | 124.83 | |
| | EVA/$CaCO_3$ | 96.80 | 148.30 | |

DSC analysis, in which diminishing nucleating efficiency of filler on PP was observed. The phase structure of ternary composites could not be changed, from a separate dispersion to full encapsulation, by simple altering the sequences in which the components were mixed. However, mixing the filler with elastomer prior to blending with PP increased the tendency of elastomer particles adhere to the filler surface.

## Acknowledgements

The authors are grateful to the National Metal and Material Technology Center (MTEC) and Institute of Science and Technology for Research and Development, Mahidol University for their financial support.

## References

[1] Stamhuis JE. Polym Compos 1984;5:202.
[2] Stamhuis JE. Polym Compos 1988;9:72.
[3] Stamhuis JE. Polym Compos 1988;9:280.
[4] Pukanszky B, Kolarik J, Lednicky F. In: Sedlacek B, editor. Polymer composites, Berlin: Walter de Gruyter, 1986 (553pp.).
[5] Kolarik J, Lednicky F. In: Sedlacek B, editor. Polymer composites, Berlin: Walter de Gruyter, 1986 (537pp.).
[6] Pukanszky B, Tudos F, Kolarik J, Lednicky F. Polym Compos 1990;11:98.
[7] Kolarik J, Lednicky F, Jancar J, Pukanszky B. Polym Commun 1990;31:201.
[8] Kolarik J, Jancar J. Polymer 1992;33:4961.
[9] Kolarik J, Pukanszky B, Lednicky F. Compos Polym 1990;2:271.
[10] Marosi Gy, Bertalan Gy, Rusznak I, Anna P. Colliods Surf 1986;23:185.
[11] Kosfeld R, Schaefer K, Kemmer EA, Hess M, Theinsen A, Uhlenbroich TH. In: Ishida H, editor. Controlled interphases in composite materials, Amsterdam: Elsevier, 1990 (385pp.).
[12] Schaefer K, Hess M, Kosfeld R, Uhlenbroich TH. Kunststoffe 1990;80:19.
[13] Schaefer K, Theinsen A, Hess M, Kosfeld R. Polym Engng Sci 1993;33:1009.
[14] Dao KC, Hatem RA. SPE ANTEC Tech Papers 1984;30:198.
[15] Hornsby PR, Premphet K. J Appl Polym Sci 1998;70:587.
[16] Comitov PG, Nicolova ZG, Simeonov IS, Naidenova KV, Siarova AD. Eur Polym J 1984;20:405.
[17] Wu S. J Macromol Sci C: Rev Macromol Chem 1974;10:1.
[18] Scott C, Ishida H, Maurer FHJ. J Mater Sci 1991;26:5708.
[19] Wu S. Polymer interface and adhesion. New York: Marcel Dekkar, 1982.
[20] Pukanszky B. Polypropylene structure, blend and composites. In: Karger-Kocsis J, editor. Composites, vol. 3. London: Chapman & Hall, 1995. p. 26.